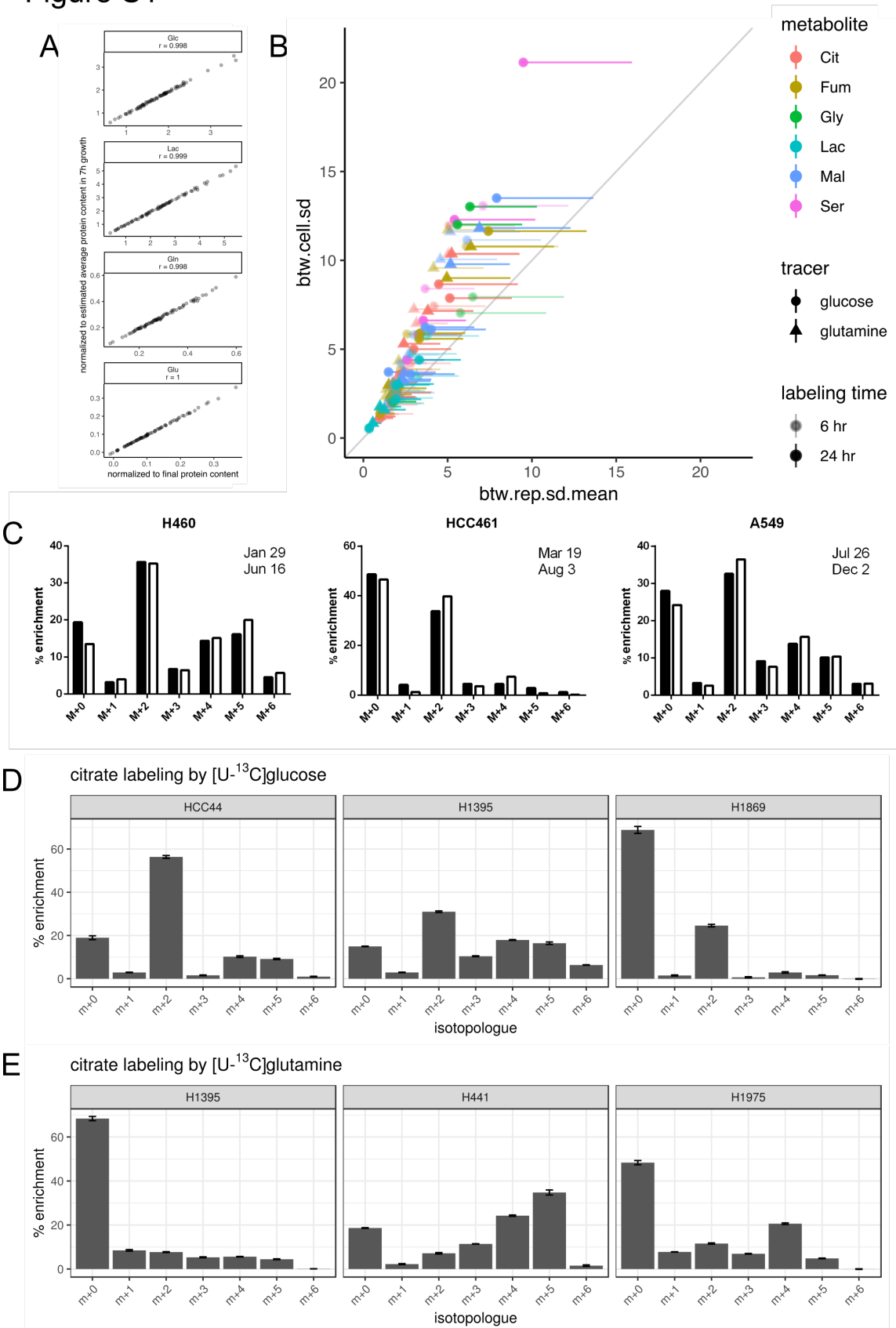


Figure S1



**Figure S1. Related to Figures 1 and 2. Low levels of variation among biological replicates and high levels of cell-autonomous metabolic diversity among cell lines.**

(A). Agreement of nutrient utilization/secretion data normalized by final protein content or by estimated average protein content during 7h growth.

(B). Scatterplot comparing the averaged variations among biological replicates for the same cell line (x-axis values) and variations among all cell lines (y-axis values) for isotopologue enrichment data from  $^{13}\text{C}$  tracing experiments. For each isotopologue, the color represents the metabolite of interest, shape represents the tracer, and transparency represents the labeling time. Standard deviations were calculated as variation estimates; the standard deviations of the between-replicate standard deviations were also calculated and plotted as horizontal tails extending to the right for each isotopologue.

(C). Mass isotope distribution (MID) of citrate labeled by  $[\text{U-}^{13}\text{C}]$ glucose for 6 hours in biological replicates of 3 cell lines. For each cell line, the replicate experiments were conducted with gaps of several months in between.

(D and E). Distinct MID pattern of citrate for different cell lines, labeled by  $[\text{U-}^{13}\text{C}]$ glucose (D) or  $[\text{U-}^{13}\text{C}]$ glutamine (E) for 6hr, indicating the striking diversity of labeling patterns among these cell lines. Data are represented as mean  $\pm$  SEM.

Figure S2

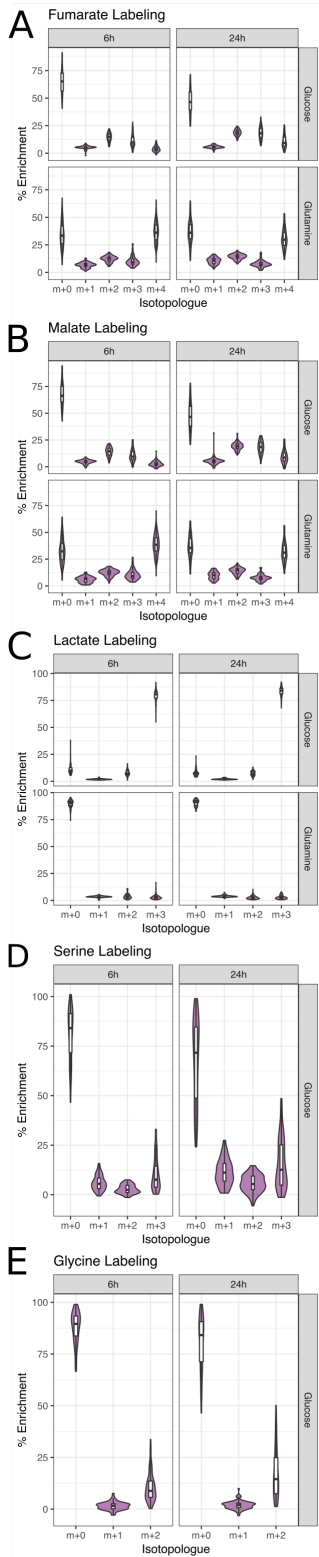


**Figure S2. Related to Figure 2. Mass isotopologue distribution and variation for selected metabolites from [U-<sup>13</sup>C]glucose or [U-<sup>13</sup>C]glutamine labeling.**

(A-E). Violin plots showing mass isotopologue distribution in fumarate (A), malate (B), lactate (C), serine (D) and glycine (E).

(F). Variance of different isotopologues.

Figure S3

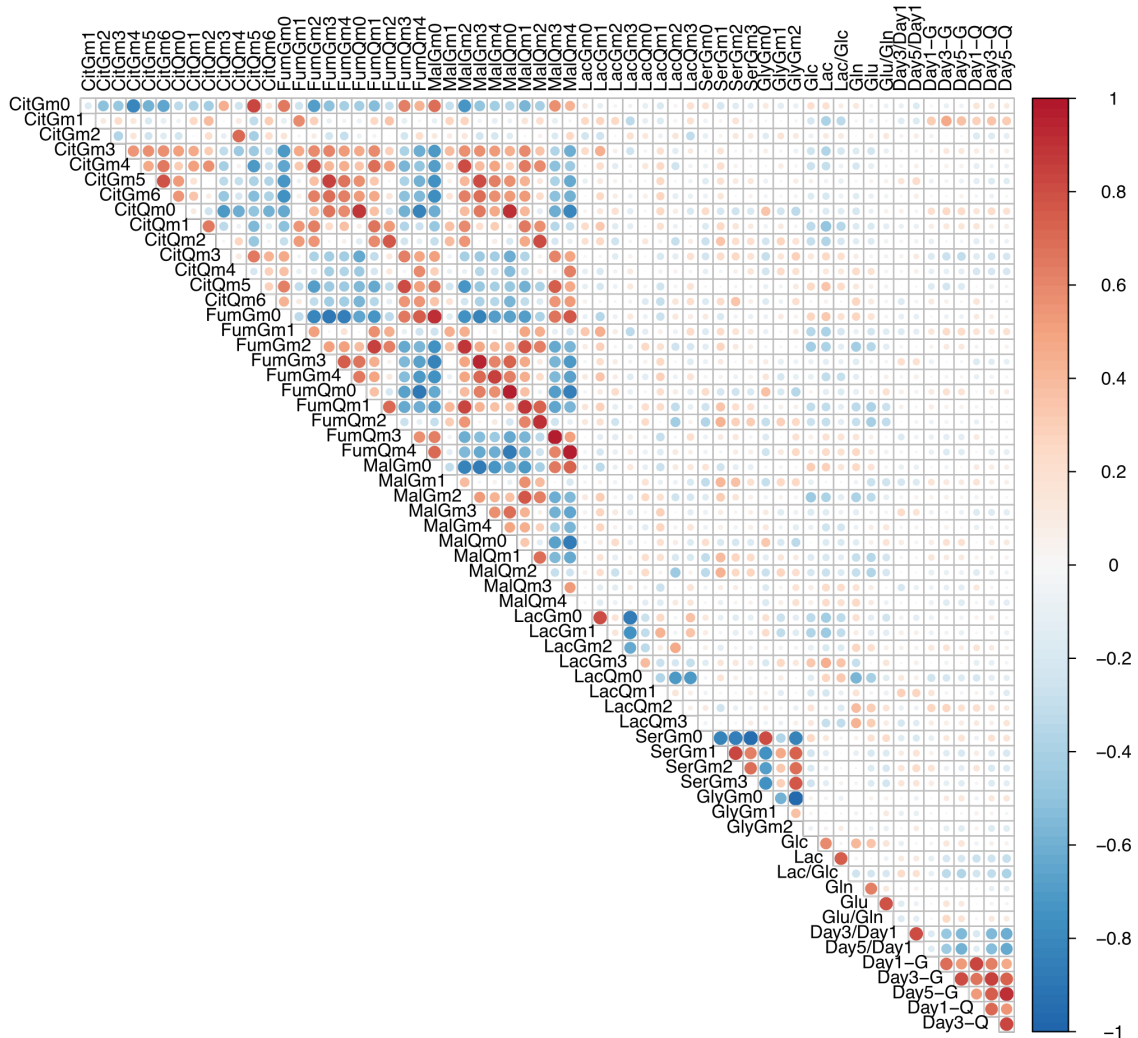


**Figure S3. Related to Figure 1. Correlation heatmap visualizing pairwise Pearson correlations among all metabolic features**

These correlations are based on isotopologue fractions from  $^{13}\text{C}$  tracing experiments at 6h and at 24h as well as features from nutrient utilization, cell growth and nutrient dependency. Larger sizes and darker shades of the circles reflect more significant correlations. Red circles indicate positive correlations and blue circles indicate negative correlations.

Figure S4

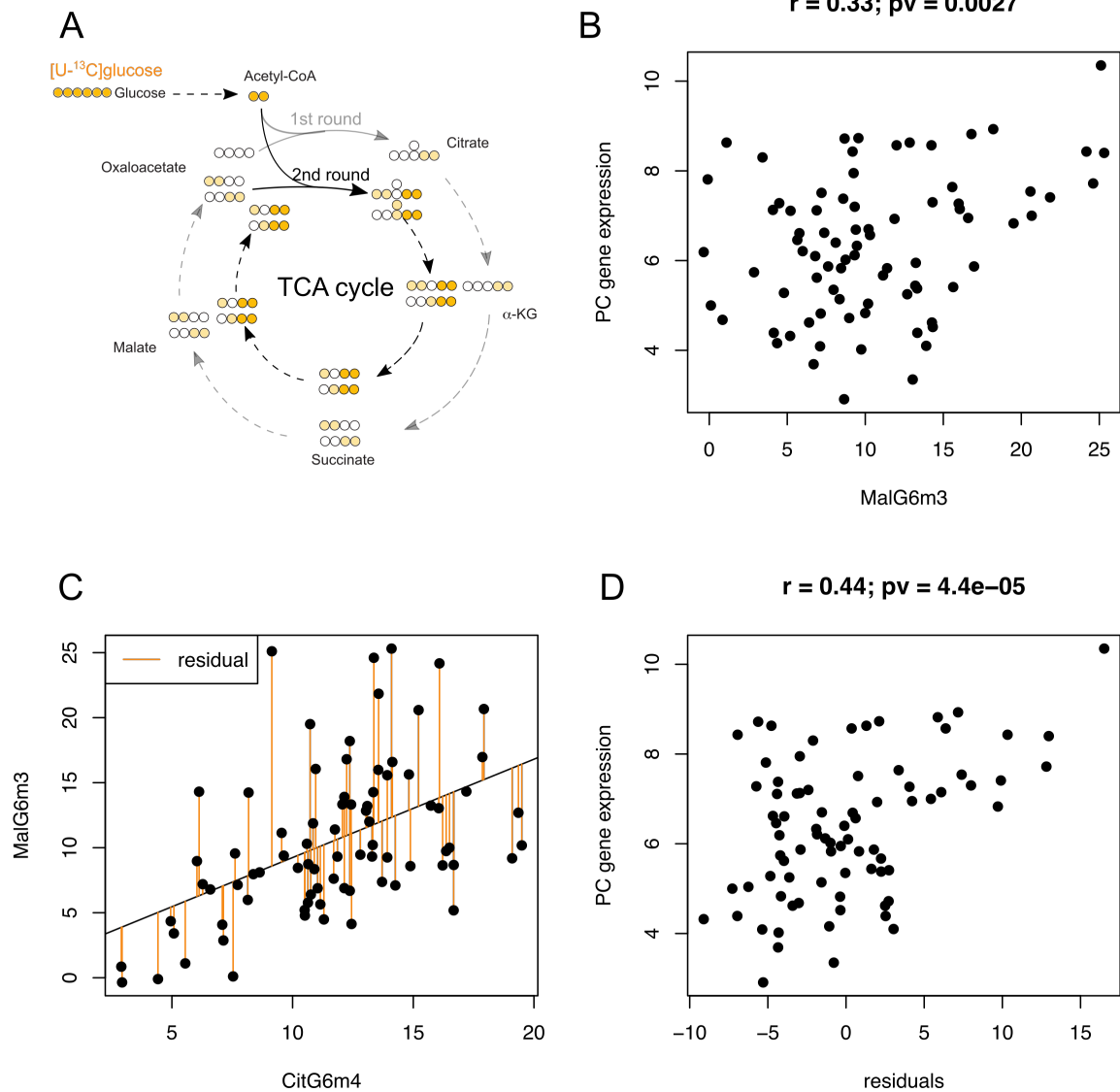


**Figure S4. Related to Figure 3. Estimation of pyruvate carboxylation dependent anaplerosis after  $[U-^{13}C]$ glucose labeling**

(A). Malate m+3 can be generated from  $[U-^{13}C]$ glucose after two rounds of the TCA cycle. This confounds the interpretation of Malate m+3 as an indicator of pyruvate carboxylase contribution. Citrate m+4 is the nearest detectable TCA cycle intermediate in this route that cannot be reversibly generated from malate m+3. Therefore it might serve as a predictor for Malate m+3 generated through this pathway.

(B). Scatter plot showing correlations between *PC* gene expression and MalG6m3. The correlation coefficient and p-value in the title are based on Pearson correlation.

(C). Residuals from regressing MalG6m3 on CitG6m4 might represent MalG6m3 produced independently from the pathway in (A), the majority of which likely arises from pyruvate carboxylation.

(D). Scatter plot showing correlations between *PC* gene expression and residuals from regressing MalG6m3 on CitG6m4. The correlation coefficient and p-value in the title are based on Pearson correlation.

Figure S5

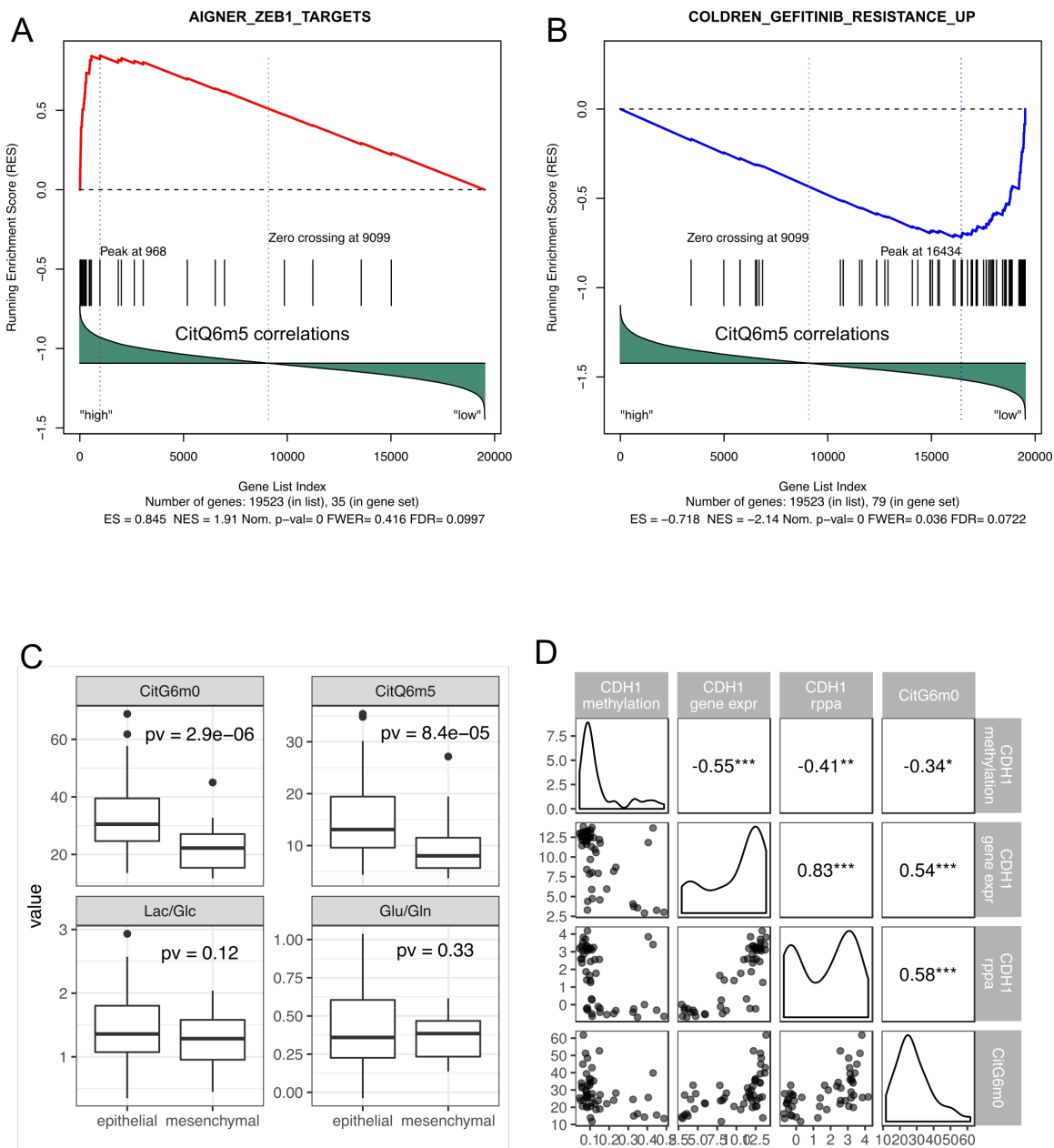


**Figure S5. Related to Figure 5 and Table S4. The GDRC phenotype is associated with epithelial state**

(A-B). Gene Set Enrichment Analysis (GSEA) identified CitQ6m5 as positively correlated with ZEB1 target genes (A) and negatively correlated with Gefitinib resistance genes (B).

(C). CitG6m0 and CitQ6m5 are significantly different between the epithelial and mesenchymal groups, whereas similar levels of Lac/Glc and Glu/Gln were observed in the two groups. Epithelial and mesenchymal group classification was based on hierarchical clustering with the EMT gene expression signature in Figure 5D. p-values from t-test are provided.



(D). Scatterplot and density plots with pairwise Pearson correlations among *CDH1* methylation, *CDH1* gene expression, *CDH1*-encoded E-cadherin expression and CitG6m0. \*\*\*,  $p \leq 0.001$ ; \*\*,  $p \leq 0.01$ ; \*,  $p \leq 0.05$ .

Figure S6

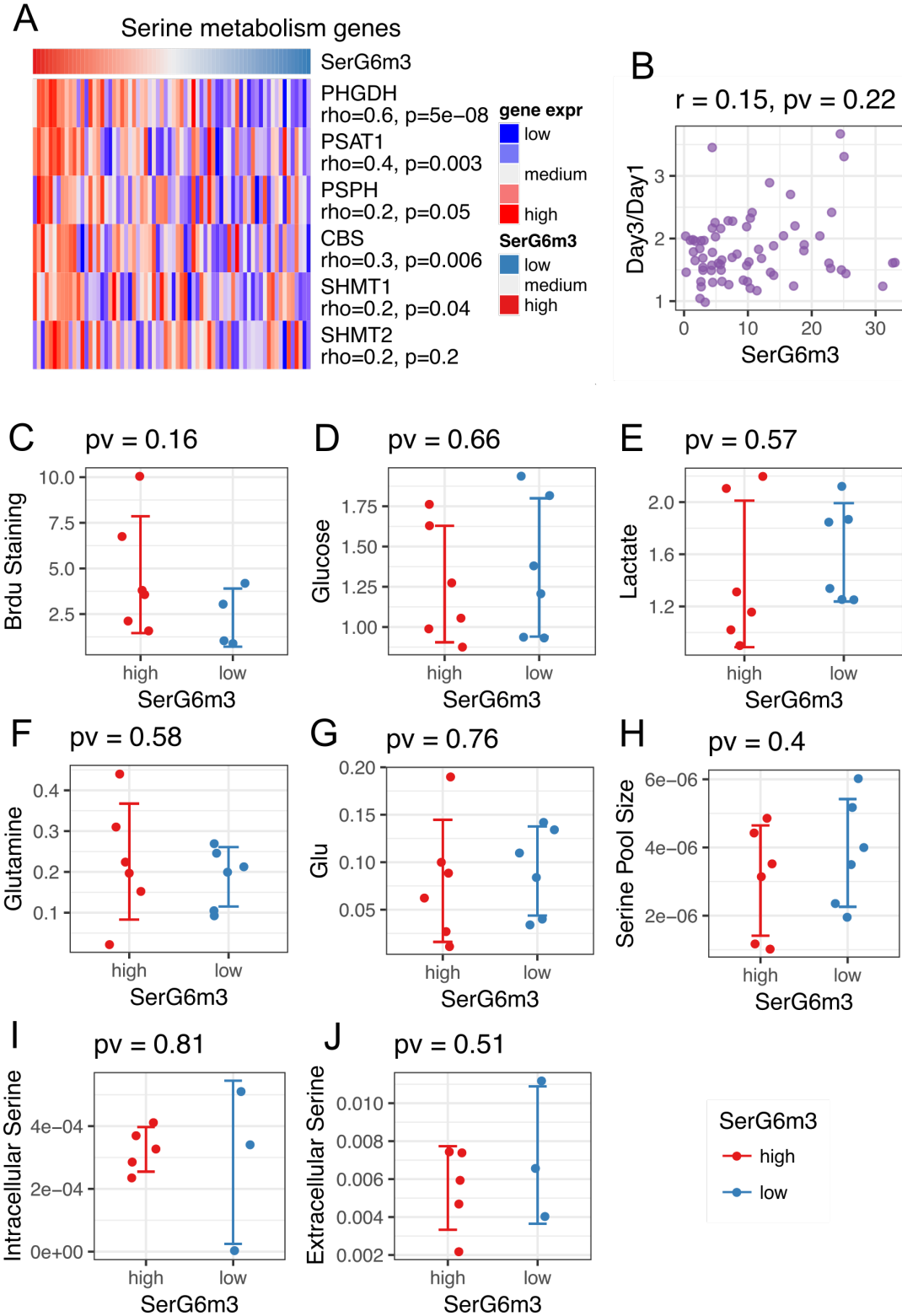


**Figure S6. Related to Figure 6. Association between SerG6m3 and serine metabolism genes and comparison of various metabolic features in selected SerG6m3-high and -low cells**

(A). Heatmap showing expression of selected genes involved in serine metabolism. Correlation coefficients and p-values from Spearman correlations between gene expression and SerG6m3 are provided.

(B). Non-significant correlation between SerG6m3 and cell growth feature Day3/Day1.

(C-J). Insignificant results from comparing BrdU staining (C), glucose uptake (D), lactate secretion (E), glutamine uptake (F), glutamate secretion (G), intracellular serine pool size inferred from GC-MS (H), intracellular (I) or extracellular (J) serine concentrations measured by HPLC in SerG6m3-high and -low cell lines.

Each dot represents average from triplicates for a single cell line; error bars denote mean  $\pm$  SD for each group.